Recognition of Distributed Combustion Regime From Deep Learning

Rishi Roy
Department of Mechanical Engineering,
University of Maryland,
College Park, MD 20742
e-mail: rroy1235@umd.edu

Ashwani K. Gupta
Professor
Department of Mechanical Engineering,
University of Maryland,
College Park, MD 20742
e-mail: akgupta@umd.edu

Swirl-assisted distributed combustion was examined using a deep-learning framework. High intensity distributed combustion was fostered from a 5.72 MW/m^3 *atm thermal intensity swirl combustor (with methane fuel at equivalence ratio 0.9) by diluting the flowfield with carbon dioxide. Dilution of the flowfield caused reduction of global oxygen (%) content of the inlet mixture from 21% to 16% (in distributed combustion). The adiabatic flame temperature gradually reduced, resulting in decreased flame luminosity and increased flame thermal field uniformity. Gradual reduction of flame chemiluminescence was captured using high-speed imaging without any spectral filtering at different oxygen concentration (%) levels to gather the data input. Convolutional neural network (CNN) was developed from these images (with 85% of total data used for training and 15% for testing) for flames at* $O_2 = 16\%$, *18%, 19%, and 21%. Hyperparameters were varied to optimize the model. New flame images at* $O_2 = 20\%$ *and 17% were introduced to verify the image recognition capability of the trained model in terms of training image data. The results showed good promise of developed deep-learning-based convolutional neural network or machine learning neural network for efficient and effective recognition of the distributed combustion regime.* [DOI: 10.1115/1.4053616]

Keywords: air emissions from fossil fuel combustion, energy conversion/systems, energy systems analysis, fuel combustion, natural gas technology

Introduction

Development of precise control systems is an important requirement for modern low emission gas turbines for stable and efficient operation. Precision of such systems can be achieved with increasing autonomous controls of the combustor. Artificial intelligence and machine learning-based predictions are now popular in the scientific community for developing such autonomous control systems [1]. Deep learning has further aided to the efficiency of predictions as compared with the conventional artificial intelligence techniques. Recent trends in combustion research involve investigating deep learning along with computer vision to detect different combustion modes [2]. Such deep-learning models may use image, audio, and various other time-series data as inputs. There is a growing demand of utilizing deep learning for the classification and recognition of flame characteristics and combustion states related to high intensity gas turbine combustion [3].

The training dataset for this deep-learning work was collected from the distributed combustion experiments performed in a lab-scale swirl combustor (with nominal 45 deg swirl angle). The fundamental requirement of the distributed combustion is that the hydrodynamic time scale in distributed combustion should be much shorter than the chemical time scale (such that the Damkohler number is <1). High intensity distributed combustion was fostered from a 5.72 MW/m^3 atm methane swirl flame by diluting the main airstream with carbon dioxide [4,5]. With gradual dilution of airstream, the inlet oxygen concentration reduced from 21% (in traditional swirl combustion) to 16% in distributed combustion. Better mixing of fuel and air was achieved by the dilution of airstream that primarily reduced the flame speed as well as the overall flame temperature. Reduction in flame temperature promotes lower chemiluminescence intensity and the reaction occurred in much wider volume in distributed combustion resulting in a volumetric reaction zone. In contrast, the conventional swirl flame existed with a short reaction zone downstream of the nozzle exit. Hence, the visible appearance of the distributed reaction zone differed significantly from the conventional swirl flames. The distributed combustion was fostered by manually adding the diluent CO_2 with the airstream using flow controllers in the lab-scale high intensity combustor. However, advanced autonomous control systems are needed to make experiments accurate and faster by reducing manual intervention. Autonomous controls are also essential for deploying this technology in practical gas turbines for enhanced performance, fuel savings, and reduced pollutants emission.

This paper primarily focuses on how developing autonomous control systems for distributed combustion can be achieved using image-based recognition of combustion states using the flame chemiluminescence, shape, and standoff characteristics. Deep-learning-based convolutional neural network [6] or CNN is an efficient modeling technique, generally used for image classification and recognition tasks. Neural network model is a popular artificial intelligence technique that finds widespread application in regression and classification tasks. The CNN is a very useful model like the artificial neural network model [7] that is used in various fields such as medical imaging, traffic signs detection [6], remote sensing images classification, and autonomous driving tasks. In this research, detection of the onset of swirl-assisted distributed combustion was performed using image recognition techniques. The primary objective of this study was to showcase how image (of different flames) classification and recognition can be performed using CNN to generate combustor control based on model's decision making. The use of the teachable machine [8] was highlighted to develop small image recognition models without requiring complicated deep-learning models. Optimization was performed by varying different hyperparameters of the model such as learning rate (LR), batch size, and epochs. These parameters determine the structure of any neural network and also strongly influence the model training. Effectiveness of such modeling was verified by checking its capability in recognizing new flame images by the

Contributed by the Advanced Energy Systems Division of ASME for publication in the Journal of Energy Resources Technology. Manuscript received December 12, 2021; final manuscript received January 17, 2022; published online February 16, 2022. Editor: Hameed Metghalchi.

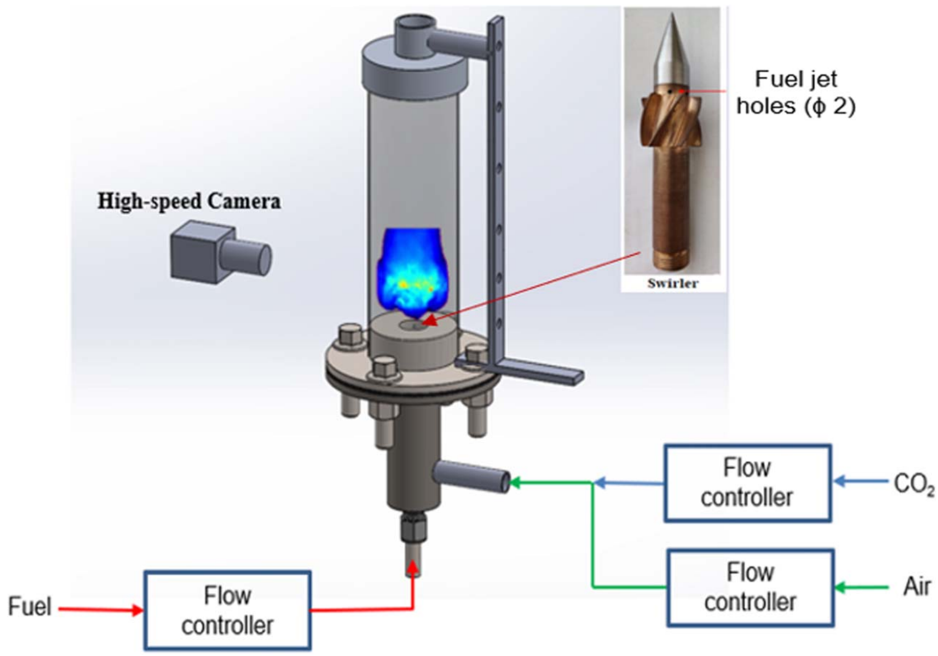

Fig. 1 3D model of the swirl burner

current CNN. New flame images were introduced (which were not used for model training) to verify model's capability of image recognition. This research helps in exhibiting the ways of autonomous transition to distributed combustion mode from conventional air-swirl combustion using image-based classification and pattern recognition.

Experimental

Data-driven image classification model was developed using the chemiluminescence images of the distributed reaction zones. Distributed combustion was established from a lab-scale methane swirl flame (5.72 MW/m^3 atm thermal intensity) by diluting the main airstream with CO_2. The current swirl-burner configuration is exhibited in Fig. 1. The inlet diameter of the burner nozzle exit (D) is 20 mm and the nozzle was integrated to a 60 mm internal diameter and 200 mm long external quartz tube. The current swirl-assisted burner used a swirler with a nominal swirl vane-angle of 45 deg. The current swirler configuration provided a calculated swirl number of −0.77 [9]. Chemically pure grade methane and hydrogen were used as the fuel. These gases were metered using AALBORG gravimetric flow controllers (with ±1.5% full scale reading, repeatability ±0.25% full scale reading) with the scale being 0–15 standard liters per minute (SLPM). The flowrate of primary airstream was controlled using OMEGA flow controller with an accuracy of ±0.8% of reading + 0.2% of full scale in full scale of 1000 SLPM. Table 1 shows the experimental conditions.

Table 1 Experimental conditions for the current study

Air (L/min)	CH_4 (L/min)	Diluent CO_2 (L/min)	Global oxygen concentrations (%)
52.20	4.93	0	21
		2.61	20
		5.49	19
		8.70	18
		12.28	17
		16.31	16

High-speed imaging of broadband flame chemiluminescence (captured at 2000 frames/s) was performed at different global oxygen concentration levels ($O_2 = 16–21\%$) corresponding to various dilution levels. This framing rate was chosen to keep a good signal-to-noise ratio while having sufficient data for modeling. No spectral filtering was applied to capture the visible broadband light emission from the flames. This is also important for developing a simple image-based model (without needing any particular spectral filtering) capable of detecting various combustion regimes. The collected images at different O_2 concentrations (corresponding to different dilution levels) were used for training the CNN model. These training data are essentially labeled datasets containing the labels of different O_2 levels.

Fundamentals of the Current Model Training

Basic Concept of Convolutional Neural Network. The convolutional neural network (CNN) model was developed from the acquired chemiluminescence image data using conventional swirl combustion and distributed combustion hardware devices. Teachable machine by the Google Creative Lab was used extensively for the current CNN modeling. Teachable machine is based on MobileNet, which aims to efficiently develop light weight deep-learning models for mobile applications using depth-wise separable convolutions [10]. While the MobileNet focuses on small model development, the teachable machine depends on transfer learning technique [11,12]. Transfer learning is efficient in transferring the knowledge from a pretrained model to another model (generally of higher complexity) to be trained using the new available data. Transfer learning eliminates the requirement of initiating a fresh learning scheme every time with different datasets. The mathematical background of such learning was explained by Rehman [3]. For a specific domain $D = \{X, P(X)\}$ with X as the feature space and $P(X)$ as marginal probability such that $P(X) = \{x_1, x_2, \ldots, x_n\}$ for $xi \in X$. With such domain definition, a task T can be defined as $T = \{y, P(y|X)\} = \{y, \eta\}$, where η is the objective function which can be denoted by $P(y|X)$ as well. Now, if Dt and Tt represent the target domain and respective target task then Ds and Ts be the source domain with respective source tasks. The transfer learning aims at learning the target probability distribution $P(yt|Xt)$ in Dt with information gained from Ds and Ts (Ds ≠ Dt or Ts ≠ Tt).

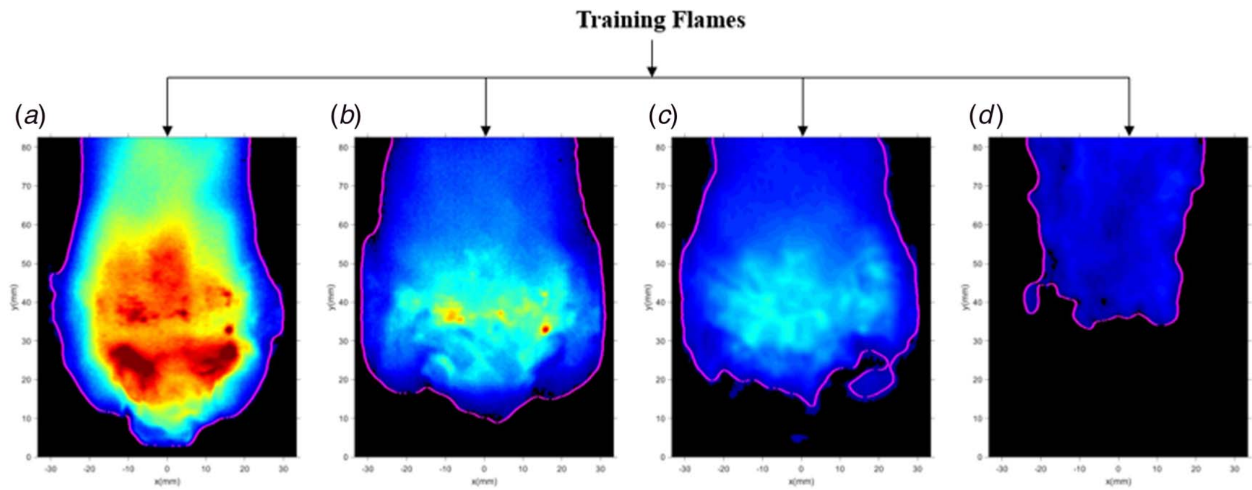

Fig. 2 Training flames at (*a*) $O_2 = 21\%$, (*b*) $O_2 = 19\%$, (*c*) $O_2 = 18\%$, and (*d*) $O_2 = 16\%$ concentrations for the current computer vision model

Table 2 The loss values corresponding to the various learning rates, epochs, and batch sizes considered

Learning rate	Batch size	Epochs	Loss
0.0001	16	20	0.004
0.001	16	20	0.00019
0.01	16	20	0.000105
0.01	16	50	0.0001002
0.01	16	100	0.00010074
0.01	32	50	0.0001053
0.01	64	50	0.00011
0.1	16	20	6.907
1.0	16	20	4.65

Basic Concept of MobileNets. The current CNN model was trained with image data for flames at $O_2 = 21\%$, 19%, 18%, and 16%. In each category, 300 chemiluminescence images (acquired at a rate of 2000 frames/s) were used for model training. Developing any good prediction model depends largely on model optimization scheme. Thus, model optimization was given importance in the current study.

The optimized classification model was chosen by repeated training of the model with hyperparameters variation (such as learning rate, batch size, and epochs). Image resizing was performed to convert the input images (of dimension 1280×720 pixels) dimension to at least 224×224 pixels and then normalized. Resizing is useful in developing a flexible neural network model capable of recognizing images of different sizes without affecting the computational efficiency. These resized images were converted into array before initiating the prediction task for image recognition. Verification of image recognition capability of the model was tested by introducing new flame images. The optimized model was used to recognize the new flame images with original 20% and 17% O_2 to verify the capability of the current model.

Results

Collecting the test data and label them individually is essential to such model development. Flame images were collected using high-speed imaging of chemiluminescence signatures at different dilution levels. The training process was performed using four different flames: conventional swirl flame (at $O_2 = 21\%$), and three CO_2 diluted flames at $O_2 = 19\%$, 18%, and 16%, which were labeled as corresponding to their O_2 concentration levels. The training flames are exhibited in Fig. 2. These images showed different visible appearance of the reaction zone shape, chemiluminescence intensity, and standoff heights from the combustor base location.

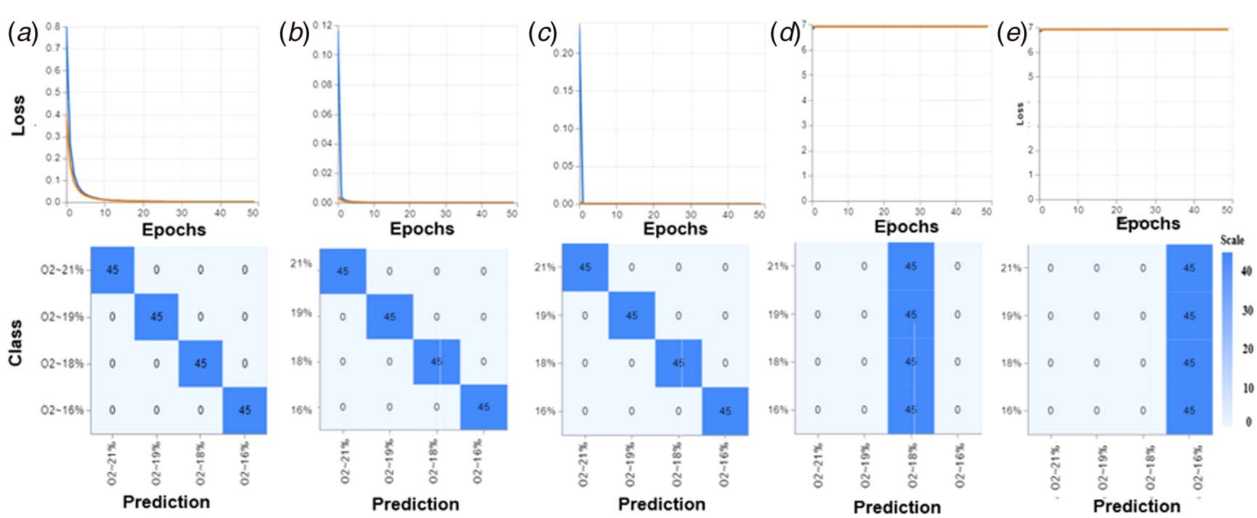

Fig. 3 Variation of loss (top row) and the confusion matrix (bottom row) for learning rates: (*a*) 0.0001, (*b*) 0.001, (*c*) 0.01, (*d*) 0.1, and (*e*) 1

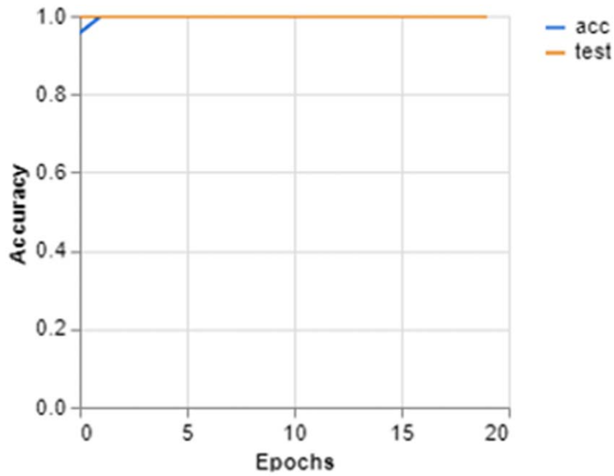

Fig. 4 Accuracy variation with epochs for the training dataset

Hence, such an image set is considered ideal for model training. A total of 300 instantaneous images were used to train the images in each category resulting in 1200 total images for the four flames used for training. Training was carried out using 85% of the total data while the testing used 15% of the data. While training the model, different learning rates (LR = 0.0001, 0.001, 0.01, 0.1, 1.0), epochs (20, 50, 100), and batch sizes (16, 32, 64) were tested to generate the best model. Generally, the best model was decided based on accuracy and loss during training. The accuracy of any CNN is defined as

$$\text{Accuracy} = \frac{\text{Number of correct predictions}}{\text{Total number of predictions made}} = \frac{\text{TP} + \text{TN}}{\text{TP} + \text{TN} + \text{FP} + \text{FN}}$$

where TP, TN, FP, and FN stand for true positive, true negative, false positive, and false negatives, respectively.

The loss in this case is the cross-entropy loss that is generally used in multiclass classification tasks [13]. The binary cross-entropy loss is defined as the negative sum of the loss of corrected predicted probabilities.

Effect of Variation of Different Learning Rates on Flame Classification. Different learning rates have been tested to investigate the performance of model training and accuracy of image recognition. The variation in loss function with respect to epochs for different LR has been tested to check the best training condition to achieve a lower number of epochs as well as the lowest loss value. The choice of the best working model was made based on the optimized loss value (of the testing data) and the number of training epochs. Table 2 outlines the loss values corresponding to various learning rates, epochs, and batch sizes considered.

The confusion matrix [14] was plotted for all these cases to verify the performance of the trained model in flame image recognition. Figure 3 compares the variation of loss and the corresponding confusion matrix at different learning rates.

As observed, the loss function gradually converged for LR = 0.0001 compared with the other learning rate cases. However, this case required more epochs to converge to the lowest possible loss. The cases with LR = 0.001 and 0.01 converge with lower epochs. The higher LR cases (0.1 and 1) converge quickly; however, these cases include very high loss values. The bottom row of Fig. 3 shows the confusion matrices for the different LR cases considered during this study. As observed, the LR = 0.0001, 0.001, and 0.01 cases predicted different flame classes (at O_2 = 21%, 19%, 18%, and 16%) very well. This is because all the testing samples (that is 15% of 300 total cases = 45 cases) were predicted as true positive (TP) for every class considered for training. For LR = 0.1 and 1, different classes were not predicted properly as seen from Fig. 3. This is because the flame classes at O_2 = 21%, 19%, 16% and O_2 = 21%, 19%, 18%, respectively, were not

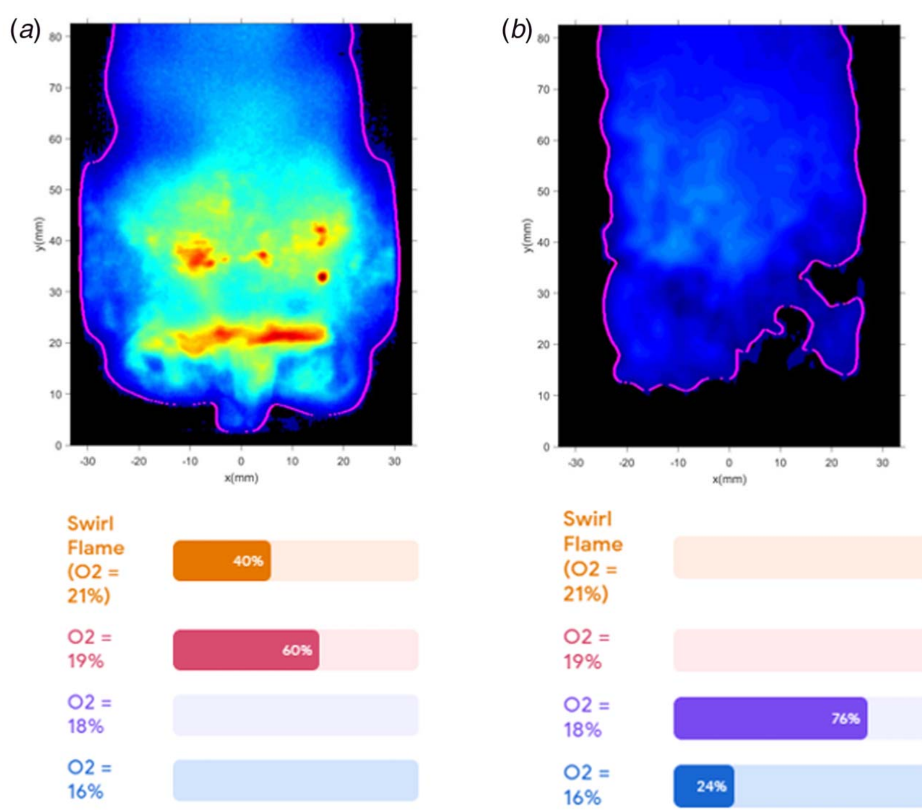

Fig. 5 Model-based image recognition: (a) O_2 = 20% and (b) O_2 = 17%

predicted for LR = 0.1 and 1 as observed from the confusion matrix. Additionally, the loss of classification for these cases was significantly higher than the lower LR cases. Thus, the lower LR values were more favorable for the current flame image classification task. To receive the lowest loss as well as faster convergence of the CNN model, the LR = 0.01 was accepted as the optimized model for the current study. Hence, the model with LR = 0.01 was utilized for further modeling and detection of new flame images in this current study.

Table 2 also confirms that the lowest loss was observed with a learning rate of 0.01, batch size 16, and epoch 50. The model with epoch 20 (with a learning rate of 0.01, batch size 16) can also be used as the loss is comparable to that of the one with epochs 50. However, for smaller dataset, like the current one, the time of convergence is not much higher than that with epoch 20 case. Hence, the model with epoch 50 was considered for this study. Figure 4 shows the variation of accuracy with epochs for the training of flame dataset with a learning rate of 0.01, batch size 16, and epoch 50. As observed the model accuracy reached near 1 at a very early stage of model training (∼epochs 2). The model training was still performed until epochs 20 to confirm the convergence of the model. Additionally, the loss function (in Fig. 3) did not rise after reaching the minimum value, so that the model was not overfitted. This was also verified by training the model for longer time that showed consistent nature of the loss function.

Next, the main task of developing this image classification model was to recognize and classify the image at its given O_2 level when any new image is introduced. The entire training process runs internally in teachable machine like a "black box" and performs the image recognition task based on the input dataset. This model characterizes any given image in terms of the test image categories. The recognition task is shown by displaying what percentage of contribution from each input image categories are contained by the image under verification. This is logical as the developed model was not expected to have the knowledge of the exact image label and should only predict the similarity of any image with the input image classes. Figure 5 demonstrates such prediction for the flames at $O_2 = 20\%$ and 17% in terms of the input images (at $O_2 =$ 21%, 19%, 18%, and 16%). The results showed that the current model predicted a combination of 60% characteristics from the $O_2 = 19\%$ flame and 40% characteristics from the $O_2 = 21\%$ conventional swirl flame for the flame at $O_2 = 20\%$ under verification. This is reasonable as this flame closely resembles the shape of flame at $O_2 = 21\%$ while the chemiluminescence intensity is very similar to the flame at $O_2 = 19\%$. The prediction of this model for the flame originally at $O_2 = 17\%$ showed 76% characteristics from the $O_2 =$ 18% reaction zone and 24% characteristics from the $O_2 = 16\%$ reaction zone. This is attributed to the fact that the shape and chemiluminescence intensity of the reaction zone at $O_2 = 17\%$ had relatively higher similarity with that of the $O_2 = 18\%$ reaction zone than the $O_2 = 16\%$ (which had a relatively higher standoff height).

Such predictions slightly varied with different instantaneous images. Hence, the current model exhibited efficient recognition capability for the flames (mainly in distributed combustion) under study. Furthermore, the model development can be performed with the acoustic signals acquired at various O_2 concentrations to make this technique more feasible for characterization of distributed combustion. The results presented here are of significant importance in swirl combustion and distributed combustion [15,16].

Conclusions

Swirl-assisted distributed reaction zones were classified and recognized using deep-learning-based convolutional neural network (CNN) framework. Distributed combustion regime was established from a 5.72 MW/m^3 atm thermal intensity swirl flame with methane (at equivalence ratio 0.9) by CO_2 dilution of the inlet air stream. Such dilution produced gradual reduction of flame chemiluminescence and broadening of reaction zones. The chemiluminescence images at different dilution levels ($O_2 = 21\%$, 19%, 18%, and 16%) were used for CNN model development using various model hyperparameters such as learning rate, batch size, and epoch. The model with a learning rate of 0.01, batch size 16, and epoch 50 was found to be optimal. While learning rates below 0.01 took higher epochs to converge, learning rates greater than 0.01 produced much higher loss value that are undesired. The trained model recognized new flame images at O_2 levels 20% and 17% very well. Such recognition was performed based on chemiluminescence signature, flame shape, and standoff distances of the new images introduced with respect to the training images. This study assisted in image-based autonomous control system development to foster distributed combustion in lab scale without manual intervention. The results show a good promise of fostering distributed combustion in advanced high intensity gas turbines with deep-learning-based control systems to support high performance and near zero emissions.

Conflict of Interest

There are no conflicts of interest.

Data Availability Statement

The data and information that support the findings of this article are freely available.

References

[1] Kobayashi, T., Murayama, S., Hachijo, T., and Gotoda, H., 2019, "Early Detection of Thermoacoustic Combustion Instability Using a Methodology Combining Complex Networks and Machine Learning," Phys. Rev. Appl., **11**(6), p. 064034.

[2] Wang, Z., Song, C., and Chen, T., 2017, "Deep Learning Based Monitoring of Furnace Combustion State and Measurement of Heat Release Rate," Energy, **131**(1), pp. 106–112.

[3] Rehman, U. O., 2020, "Multi Task Convolutional Learning for Flame Characterization," Master's thesis, Linköping University, Linkoping, Sweden.

[4] Roy, R., and Gupta, A. K., 2021, "Experimental Investigation of Flame Fluctuation Reduction in Distributed Combustion," Exp. Fluids, **62**(4), pp. 1–17.

[5] Cellek, M. S., 2022, "Evaluation of Oxygen Enrichment Effects on Distribution Combustion Mode in a Laboratory-Scale Furnace," Int. J. Energy Clean Environ., **23**(1), pp. 19–37.

[6] Li, Q., Cai, W., Wang, X., Zhou, Y., Feng, D. D., and Chen, M., 2014, "Medical Image Classification With Convolutional Neural Network," 13th International Conference on Control Automation Robotics & Vision (ICARCV), Singapore, Dec. 12–14, pp. 844–848.

[7] Neeraj, M., Singh, B., and Kumar, A., 2021, "Performance Prediction of Innovative Solar Air Collector (ISAC) With Phase Change Material Using the ANN Approach," Int. J. Energy Clean Environ., **21**(5), pp. 65–83.

[8] Phillips, K., 2019, "Teachable Machine 2.0 Makes AI Easier for Everyone." https://blog.google/technology/ai/teachable-machine/

[9] Khalil, A. E. E., Brooks, J. M., and Gupta, A. K., 2016, "Impact of Confinement on Flowfield of Swirlflow Burners," Fuel, **184**(1), pp. 1–9.

[10] Howard, A. G., Zhu, M., Chen, B., Kalenichenko, D., Wang, W., Weyand, T., Andreetto, M., and Adam, H., 2017, "MobileNets: Efficient Convolutional Neural Networks for Mobile Vision Applications," arXiv:1704.04861 2017—arxiv.org.

[11] Pan, J. S., and Yang, Q., 2009, "A Survey on Transfer Learning," IEEE Trans. Knowl. Data Eng., **22**(10), pp. 1345–1359.

[12] Balasubramaniam, K., 2019, "Have You Taught Your Machine Yet?" Towards Data Science. https://towardsdatascience.com/have-you-taught-your-machine-yet-45540b7e646b

[13] Culfaz, F., 2018, "Transfer Learning Using Mobilenet and Keras," Towards Data Science. https://towardsdatascience.com/transfer-learning-using-mobilenet-and-keras-c75daf7ff299

[14] Dabetwar, S., Ekwaro-Osire, S., and Dias, J. P., 2019, "Damage Classification of Composites Using Machine Learning," Proceedings of the ASME 2019 International Mechanical Engineering Congress and Exposition. Volume 13: Safety Engineering, Risk, and Reliability Analysis, ASME, Salt Lake City, UT, Nov. 11–14, p. V013T13A017.

[15] Feser, J., and Gupta, A. K., 2021, "Performance and Emissions of Drop-In Aviation Biofuels in a Lab Scale Gas Turbine Combustor," ASME J. Energy Resour. Technol., **143**(4), p. 042103.

[16] Roy, R., and Gupta, A. K., 2022, "Measurement of Lean Blowoff Limits in Swirl-Stabilized Distributed Combustion With Varying Heat Release Intensities," ASME J. Energy Resour. Technol., **144**(4), p. 082301.